ELSEVIER

Catalysis Today 28 (1996) 297–303

CATALYSIS TODAY

Structure sensitivity of oxide surfaces: the adsorption and reaction of carbon monoxide and formic acid on NiO(100) and NiO(111)

Chen Xu, D. Wayne Goodman

Department of Chemistry, Texas A & M University, College Station, TX 77843, USA

Abstract

The adsorption and reaction of CO and HCOOH on the NiO(100)/Mo(100) and NiO(111)/Mo(110) surfaces have been studied using temperature programmed desorption (TPD) and high resolution electron energy loss spectroscopy (HREELS). Significant differences have been found for the two faces of NiO regarding the adsorption and reaction of HCOOH. While molecularly adsorbed formic acid is stable up to 200 K on the NiO(100) surface, formic acid decomposition to formate occurs on the NiO(111) surface at 100 K. Upon heating to 700 K, most of the formate on the NiO(111) surface dehydrogenates or dehydrates, while ~ 70% of the formate species on the NiO(100) surface desorbs as molecular formic acid. With respect to CO adsorption, the NiO(111) surface shows a slightly higher binding energy than does the NiO(100) surface.

Keywords: Structure sensitivity; Oxide surfaces; Adsorption and reaction; Carbon monoxide; Formic acid; NiO(100); NiO(111)

1. Introduction

Structure sensitivity in surface catalyzed reactions, which typically involves the breaking or making of C–C, N–N or C–O bonds [2], has been extensively researched and documented on metal surfaces [1–4]. Such reactions often occur most rapidly on open surfaces, e.g. (100) crystal planes, compared to more densely packed surfaces, e.g. (111) crystal planes. For example, the activities of various single crystal surfaces toward alkane hydrogenolysis over various transition metals are significantly different. It has been proposed that these differences in reactivities of crystal planes are responsible for the observed variations in activities as a function of metal particle size [5,6].

Structure sensitivity has also been observed on metal oxide surfaces, although this phenomenon is considerably less understood on oxides than on metal surfaces. An example of structure sensitivity in oxides is the decomposition of methanol on ZnO which depends strongly on the surface crystallographic orientation. It has also been shown that while the Zn-polar ZnO(0001) surface is quite active for methanol decomposition, the O-polar, ZnO(0001) surface is inactive [7–10]. Another example is the decomposition of carboxylic acids over TiO_2 or ZnO [11]. Depending upon the particular crystal plane, either unimolecular or bimolecular decomposition has been observed.

Recently, NiO(100) [12,13] and NiO(111) [14] surfaces have been successfully prepared in

PII S0920-5861(96)00044-2

our laboratories on the Mo(100) and Mo(110) surfaces, respectively. These well-ordered oxide films, essentially free from the problems associated with the corresponding bulk oxides resulting from poor thermal and electrical conductivity, can be studied with respect to their chemical and physical properties using an array of surface science probes. In this paper, comparative studies of CO and HCOOH adsorption on these two crystallographic NiO surfaces are reported.

2. Experimental

The experiments were carried out in a UHV chamber (base pressure of $\sim 2 \times 10^{-10}$ Torr) which has been described in detail previously [15]. Briefly, the UHV chamber was equipped with high resolution electron energy loss spectroscopy (HREELS-LK2000), Auger electron spectroscopy (AES), low energy electron diffraction (LEED), and temperature programmed desorption (TPD). TPD measurements were carried out using a line-of-sight, quadrupole mass spectrometer (QMS) and a linear heating rate of ~ 5 K/s. It is well known that the electron emission from a QMS can cause damage to a weakly bound adsorbate, thus introducing spurious decomposition products into the TPD data. To avoid such damage, the sample was biased at -100 V during the TPD experiments. The sample could be either heated to 1500 K resistively or flashed to 2200 K using an electron-beam assembly. The temperature was measured using a W–5%Re/W–26%Re thermocouple spot-welded to the sample edge. The Mo(110) and Mo(100) crystals were cleaned by annealing in 2×10^{-8} Torr O_2 at 1200 K with a subsequent flash to 2000 K. The procedure was repeated several times until no contamination could be detected with AES.

The NiO(111) or NiO(100) films were prepared by depositing Ni onto a Mo(110) or Mo(100) substrate at 400 K in a 1×10^{-6} Torr O_2 atmosphere, followed by an anneal to 550 K in 1×10^{-6} Torr O_2. The nickel source was a 0.25 mm Ni wire (99.997%, Johnson Matthey Chemical Limited) wrapped around a tungsten

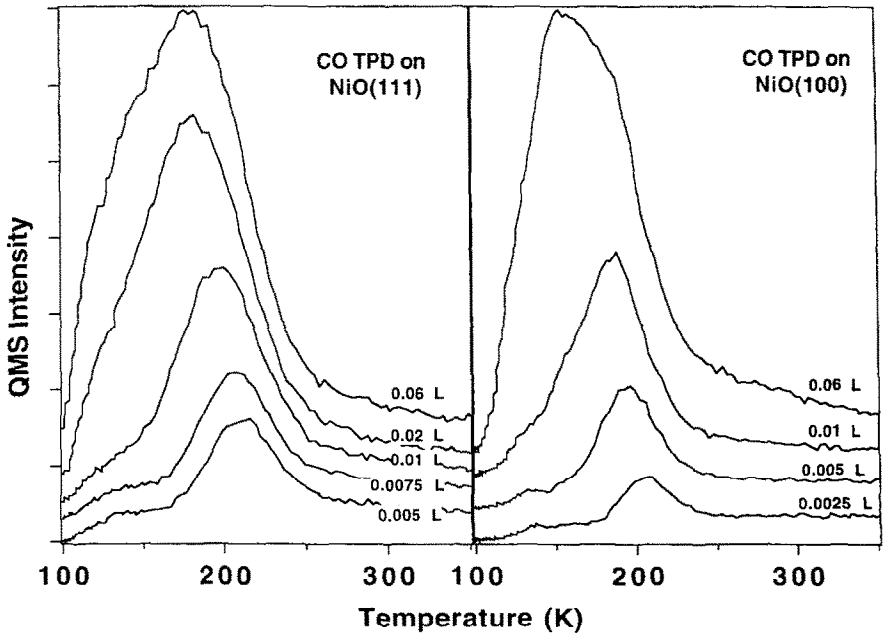

Fig. 1. Temperature programmed desorption of CO from NiO(111) and NiO(100) following various exposures. The exposures are given without correction for the local dose enhancement and gauge sensitivity.

filament; the source was extensively outgassed prior to use. The metal oxide coverage was calibrated using TPD and AES [12–14]; the evaporation rate was ~ 1 ML/min. A NiO(111) film with a thickness of ~ 30 monolayers (ML) was used in these experiments. The NiO films prepared using this procedure have been characterized previously using AES, LEED, energy loss spectroscopy (ELS) and HREELS [12–14]. It has been shown that both films have virtually identical stoichiometry, vibrational properties and electronic properties as their bulk counterparts [12–14]. The NiO films grown on the Mo(110) surface show a hexagonal LEED pattern [14], and the NiO film on Mo(100), a square LEED pattern [12,13], indicating good epitaxial growth of NiO(111) on Mo(110) [14] and NiO(100) on Mo(100) [12,13]. The NiO(111)/Mo(110) surface is likely terminated with a Ni to O ratio near one in random order [14].

Spectroscopic grade formic acid (Aldrich Chemical Company, Inc., 96%) was used after further purification in the gas-handling manifold via several freeze–pump–thaw cycles. CO (Matheson, 99.99%) was used as received without further purification. In the TPD experiments, a directional gas doser was used to introduce the formic acid and CO to the crystal surface. For the HREELS studies, the CO and HCOOH exposures were carried out via backfilling the UHV chamber. The exposures are given in Langmuir ($L = 1 \times 10^{-6}$ Torr s) without correction for the local dose enhancement and gauge sensitivity.

3. Results and discussion

Fig. 1 shows CO TPD spectra from the two NiO surfaces acquired after various CO exposures at 90 K. At a CO exposure of 0.005 L, the NiO(100) surface exhibits a desorption peak maximum at 205 K. The maxima shift toward lower temperature with increasing coverage, finally reaching 155 K at saturation CO coverage. The shift to lower binding energy with increasing coverage can be attributed either to repulsive dipole–dipole interactions between the adsorbed CO molecules or to the inhomogeneity of the CO adsorption sites. CO adsorption on a NiO(100) film grown on a Ni(100) surface has been studied by Cappus et al. [16]. A decrease in the CO binding energy with increasing coverage was also observed in this study; however, the CO desorption temperature reported by Cappus et al. was ~ 50 K lower than that found in our experiments. It is unlikely that this large discrepancy in desorption temperature is due to error in the temperature measurement. It is more likely that the difference is due to intrinsic differences in the NiO films used in the two experiments. The NiO(100) films used by Cappus et al. had a thickness of only a few monolayers. Moreover, the films were partially hydroxylated due to a restricted anneal temperature of only 600 K. The films used in our experiments had thicknesses of ~ 30 ML and were annealed to 850 K to completely dehydroxylate the surface.

The TPD spectrum of CO from the NiO(111) surface exhibits behavior very similar to that found for the NiO(100) surface. That is, a gradual decrease in the CO desorption temperature from 215 to 180 K with increasing CO coverage is observed. However, the peak width and desorption temperature of CO from the NiO(111) at certain coverages are somewhat different from the NiO(100) surface. This is seen more clearly in Fig. 2, where the TPD spectra at low CO coverages (~ 15% of the saturation coverage) are compared between the two surfaces. At low coverage, the dipole–dipole interactions are minimized and the CO-binding energy is primarily determined by the CO-surface interaction. In Fig. 2, it is apparent that the CO desorption peak is slightly broader on the NiO(111) surface compared to the NiO(100) surface. This broadening is probably due to inhomogeneities on the polar NiO(111) surface. It is noteworthy as well that the desorption peak maximum in the CO TPD from the NiO(111)

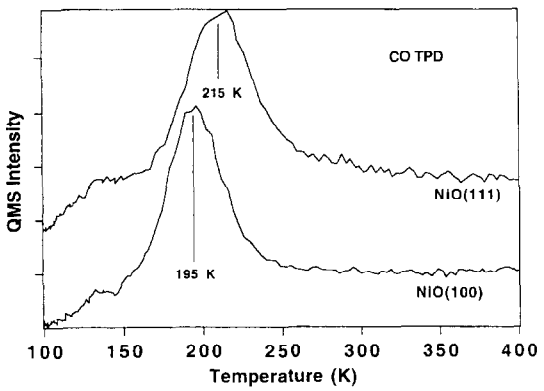

Fig. 2. Comparison of CO temperature programmed desorption between the NiO(100) and NiO(111) surfaces at a CO coverage of ~ 15% of the saturation coverage.

surface appears at a temperature ~ 20 K higher than on the NiO(100) surface, consistent with a slightly higher binding energy of CO on the NiO(111) surface compared to the NiO(100) surface. A Redhead analysis using a pre-exponential factor of 10^{13} yields a difference in binding energies of CO on NiO(100) and NiO(111) of 5.4 kJ mol^{-1}.

To estimate the CO coverage on the two NiO surfaces, CO TPD data were acquired from the clean Mo(110) surface subsequent to the removal of the NiO film. This removal was carried out by flashing the surface to 2000 K. Two peaks at 350 and 1030 K were observed in the CO/Mo(110) data, and are assigned to molecular and recombinative desorption of CO [17]. The peak area ratios among the CO TPD features for the NiO(100), NiO(111) and Mo(110) surfaces are 0.81:0.72:1.0, respectively, at saturation CO coverage, indicating that CO adsorption on the oxide surfaces is associated with majority sites rather than minority (defect) sites.

To understand the bonding mechanisms of CO on ionic oxides such as NiO and MgO, theoretical calculations have been carried out by several researchers [17–21]. These calculations suggest a dominant electrostatic interaction between CO and the NiO(100) surface with only minor contributions from σ-donation and π-back donation. Within this bonding scheme, CO interacts with the surface via an electrostatic interaction consisting of the permanent multipole moments of CO within the electric field above the surface. This attraction between CO and the surface is balanced by an electron–electron repulsive interaction, which depends on the CO–surface distance and the number of nearest neighbor O^{2-} ions surrounding the CO. The binding energy of CO is therefore directly proportional to the electric field above the surface. For NiO, a higher CO binding energy on the polar (111) surface is observed than on the nonpolar (100) surface. This is consistent with the fact that the electric field above the NiO(111) surface is larger than the corresponding field above the NiO(100) surface. However, the observed differences in the two surfaces with respect to the CO binding energies is less significant than one would predict taking into account the infinitely large electric field on the ideal-terminated polar surface. Even on the most stable octopolar reconstructed (111) surface, the electric field is higher by a factor of two compared to the nonpolar (100) surface [22]. This difference indicates that one or more other factors besides simple electrostatic interactions must be important in the bonding of CO to the polar NiO(111) surface. One possible explanation is that electron–electron repulsion between CO and the surface is larger on the (111) surface than on the (100) surface. This follows from the fact that the nearest neighbor oxygens are in the same plane as CO on the (111) surface, unlike the environment of CO on the (100) surface.

CO adsorption on the NiO(111) surface has also been studied using HREELS (Fig. 3). The HREELS spectra were acquired using a primary beam energy of 25 eV to suppress the strong phonon loss features of the NiO substrate. At low CO coverages, a peak due to the C–O stretching vibration is observed at 2190 cm^{-1}. This feature shifts to 2165 cm^{-1} as the CO coverage approaches saturation. A previous study of CO adsorbed on the NiO(100) surface has shown the CO vibrational feature to shift

from 2156 cm^{-1} at low CO coverages to 2142 cm^{-1} at saturation coverage [23]. For both NiO(110) and NiO(111), a blue shift with respect to the CO gas phase frequency (2143 cm^{-1}) is observed. This blue shift, however, is larger for the (111) polar surface than for the (100) nonpolar surface. The blue shift of CO with respect to the gas phase frequency on ionic surfaces has been explained by the formation of a σ-dative interaction between the 5σ lone pair of CO and the empty states of the metal cations [24,25]. Since the 5σ orbital is slightly antibonding in character, the donation of 5σ electron density to the surface results in a blue shift of the carbon–oxygen vibrational frequency. A recent theoretical calculation by Pacchioni et al. [19,20], however, attributes this blue shift mainly to the so-called 'wall-effect' and the interaction between the non-uniform electric field at the surface and the CO dynamic dipole. This wall-effect is believed to dominate the CO interaction with non-polar oxide surfaces and is a consequence of the molecule vibrating in the presence of the 'rigid' surface. Both mechanisms yield an increasing blue shift for a more tightly bound CO, consistent with our experimental findings for the NiO(100) and NiO(111) surfaces.

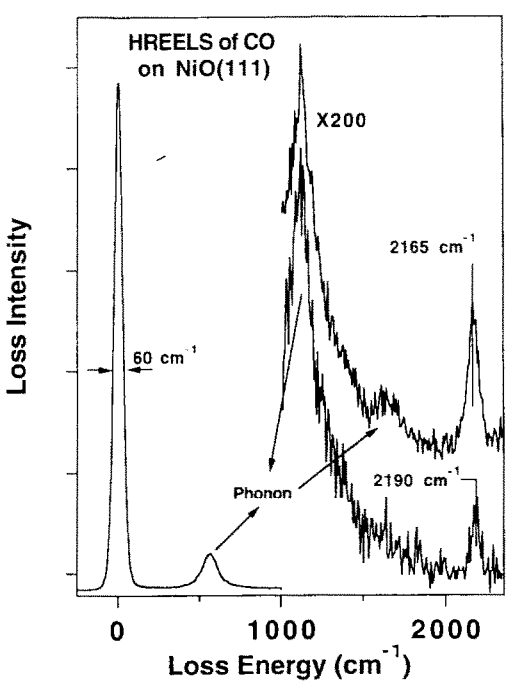

Fig. 3. High resolution electron energy loss spectra of CO adsorbed on the NiO(111) surface. The exposures were carried out via backfilling the UHV chamber to 1×10^{-8} Torr for 20 s (bottom) and 100 s (top), respectively.

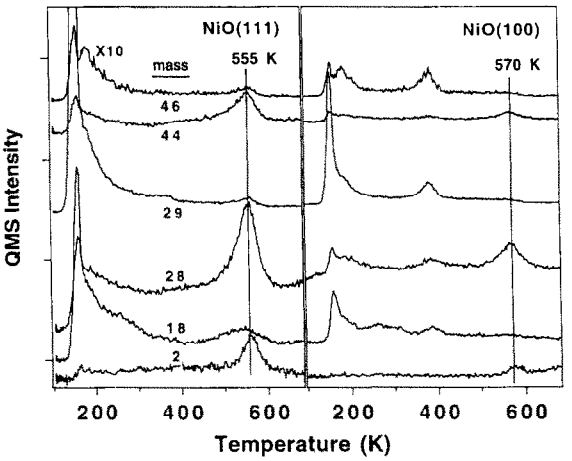

Fig. 4. Temperature programmed desorption spectra following adsorption of a saturation coverage of formic acid on the NiO(111) and NiO(100) surfaces.

Because of the demonstrated structure sensitivity of formic acid adsorption [11,26], this molecule was investigated as well on the (100) and (111) NiO surfaces. Fig. 4 compares TPD spectra acquired following formic acid adsorption on the NiO(111) and NiO(100) surfaces. Masses 29 and 46 were used to monitor the primary fragment, HCO, and the parent peak of molecular formic acid, respectively. Desorption products due to dehydration and dehydrogenation are also observed. Masses 2 and 44 follow H_2 and CO_2, respectively, and are products of formic acid dehydrogenation, while masses 18 and 28 monitor H_2O and CO, respectively. These latter two products result from formic acid dehydration. For all masses except mass 2, a sharp feature is observed at 160 K. This feature does not saturate with increasing formic acid coverage and is therefore due to desorption from a formic acid multilayer. For the NiO(111) surface, the TPD spectra above 200 K are domi-

nated by H_2, H_2O, CO and CO_2 desorption at 555 K, a temperature well above the corresponding molecular desorption temperatures. These molecules, then, must be formed in a reaction-limited process, desorbing immediately from the surface. The formation of H_2 and CO_2 suggest a facile dehydrogenation pathway; H_2O and CO follow the dehydration of formic acid. Dramatic differences between NiO(111) and NiO(100) are apparent. First, the reaction temperature for the formation of H_2, CO and CO_2 shifts to a higher temperature on the NiO(100) surface compared to the Ni(111) surface. Moreover, for the Ni(100) surface a substantial amount of molecular formic acid desorbs at 380 K. A quantitative evaluation of the individual peak areas shows that dehydration and dehydrogenation of formic acid are attenuated by ~ 70% on the NiO(100) surface compared to the NiO(111) surface. These dramatic differences in reactivity of the two NiO surfaces toward formic acid decomposition are also evident in previously reported HREELS results [12,14]. A series of HREELS spectra acquired subsequent to annealing a NiO(100) surface covered with less than a monolayer of formic acid shows that formic acid is stable up to 200 K [12]. In contrast, formic acid adsorbs dissociatively at 100 K yielding a formate species on the NiO(111) surface [14]. Two factors could contribute to the relatively high reactivity of the NiO(111) surface. First, the relative instability of the polar NiO(111) surface compared to the nonpolar NiO(100) surface will facilitate reactions that yield surface-stabilizing products. Second, the presence of neighboring Ni^{2+} sites on the (111) surface, sites that are not available on the NiO(100) surface, provide a unique reaction site for formic acid decomposition.

4. Conclusion

A comparative study of CO and HCOOH adsorption on two crystallographically different NiO surfaces has been carried out. The polar (111) surface exhibits a higher CO binding energy than does the nonpolar (100) surface. This increase in the CO bonding energy to the polar surface can be explained by the significantly different electric fields at the Ni(100) and NiO(111) surfaces. These two surfaces also exhibit markedly different reactivities toward the adsorption of formic acid. These differences in reactivity are attributed to the enhanced bond strength of the formate species on the NiO(111) surface compared to the NiO(100) surface and to the presence of neighboring Ni^{2+} sites on the NiO(111) surface.

Acknowledgements

We acknowledge with pleasure the support of this work by the Department of Energy, the Office of Basic Sciences, the Division of Chemical Sciences and by Laboratory Directed Research and Development (LDRD) funding from the Pacific Northwest Laboratory. The Pacific Northwest Laboratory is operated for the US Department of Energy by Battelle Memorial Institute under contract DE-AC06-76RLO 1830.

References

[1] M. Boudart, Adv. Catal., 20 (1969) 153.
[2] M. Boudart and G. Djega-Mariadassou, Kinetics of Heterogeneous Catalytic Reactions, Princeton University Press, Princeton, NJ, 1984.
[3] G.A. Somorjai and J. Carazza, Ind. Eng. Chem. Fundam., 25 (1986) 63.
[4] D.W. Goodman, Chem. Rev., 95 (1995) 523.
[5] G.A. Martin, J. Catal., 60 (1979) 452.
[6] D.W. Goodman, Catal. Today, 12 (1992) 189.
[7] J.M. Vohs and M.A. Barteau, Surf. Sci., 176 (1986) 91.
[8] S. Akhter, W.H. Cheng, K. Lui, and H.H. Kung, J. Catal., 85 (1984) 437.
[9] G. Zwicker, K. Jacobi and J. Cunningham, Int. J. Mass Spectros. Ion Proc., 6 (1984) 213.
[10] S. Akhter, K. Lui and H.H. Kung, J. Phys. Chem., 89 (1985) 1958.
[11] M.A. Barteau, J. Vac. Sci. Technol. A, 11 (1993) 2162.
[12] C.M. Truong, M.-C. Wu, and D.W. Goodman, J. Chem. Phys., 97 (1992) 9447.

[13] M.-C. Wu, C.M. Truong, and D.W. Goodman, J. Phys. Chem., 97 (1993) 4182.
[14] C. Xu and D.W. Goodman, Faraday Trans., in press.
[15] J.E. Parmeter, X. Jiang, and D.W. Goodman, Surf. Sci., 240 (1990) 85.
[16] D. Cappus, J. Klinkmann, H. Kuhlenbeck, and H.J. Freund, Surf. Sci., 325 (1995) L421.
[17] M.L. Colaianni, J.G. Chen, W.H. Weinberg, and J.T. Gates, Jr., J. Am. Chem. Soc., 114 (1992) 3735.
[18] M. Poehlchen and V. Staemmler, J. Chem. Phys., 97 (1992) 2583.
[19] G. Pacchioni, G. Coliandro, and P.S. Bagus, Surf. Sci., 255 (1991) 344.
[20] G. Pacchioni, G. Coliandro, and P.S. Bagus, Int. J. Quantum Chem., 42 (1992) 1115.
[21] X. Xu, X. Lue, N.Q. Wang, and Q.E. Zhang, Chem. Phys. Lett., 235 (1995) 541.
[22] D. Wolf, Phys. Rev. Lett., 68 (1992) 3315.
[23] S.M. Vesecky, X. Xu, and D.W. Goodman, J. Vac. Sci. Technol. A, 12 (1994) 2114.
[24] E.A. Colbourn and W.C. Mackrodt, Surf. Sci., 143 (1984) 391.
[25] S.A. Pope, I.H. Hiller, M.F. Guest, E.A. Colbourn and J.P. Kendrick, Surf. Sci., 139 (1984) 299.
[26] M.R. Columbia and P.A. Thiel, J. Electroanal. Chem., 369 (1994) 1.